Micro-Manufacturing

Project Report

By
Dawei Liu
Sangram Keshari Rout

Northwestern University

Contents

1. Abstract....3
2. Introduction....4
2.1. Biomimetic....4
2.2. Literature review....5
3. Equipment setup....6
3.1 ND YAG Laser machine : Class IV....6
3.2 Alicona measurement:....7
3.3 Insertion testbed:....9
3.4 Phantom Tissue....10
4. Design and machining path....11
4.1 CAD modelling and cutting analysis....11
4.2 Machining tool path....11
5. Theory....12
6. Experiment results discussion....12
7. Challenge faced during the project....14
7.1 Needle centering....14
7.2 Laser focusing....15
8. Future work....15
8.1 Finite element computation....15
8.2 P value analysis....16
8.3 Echogenic placement....17
9. Appendix....18
9.1 G Code:....18
9.2 Working log....19
10. Bibliography....19
11. Acknowledgements....20

1. Abstract

Researches has drawn inspiration from mosquito anatomy to develop Mosquito-Inspired Microneedles which are painless and have reduced drag. The principle behind is that the needle design are able to pierce through the skin at a much lower insertion force compared to standard bevel needles. The objective of our research project was to determine a serration geometry in order to pierce through the skin more easily as this would lead to lesser discomfort during the tissue extraction process. Previous studies on needle serration have tested other geometries effects on the phantom tissue. The geometry presented in this study has not been seen in any paper we have reviewed. The choice of this geometry was inspired by some of the earlier studies. In the circular profile it was determined that the tissue gets clogged in the troughs and hence the cutting edge is not effectively exposed. The proposed geometry is expected to overcome this issue. The serrations developed in this study were not perfect; the material was not ablated completely as proposed in the geometry. Nevertheless, the results demonstrate the concept that the forces and torque on operation of the needle are reduced through the micro-serrations. In the future, it is proposed that the machining operation is conduced again to have more convincing material ablation and corresponding results. Computational analysis can be run to demonstrate the concept of lowering the forces at the onset of fracture. Micro-needles are devised with surface texturing to create micro-dimples or micro-channels which aid in accurate positioning when used in conjunction with ultrasound procedures. However, these micro serration lead to undesired consequences such as patient discomfort sue to the increased friction. It is also proposed that echogenic needles which require micro serrations, should be optimally placed so that they are functional for positioning yet reduce the friction forces can be formed as part of a future study.

2. Introduction

2.1. Biomimetic

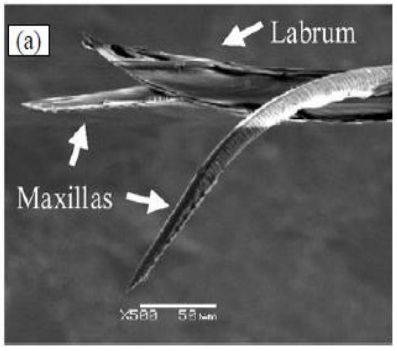

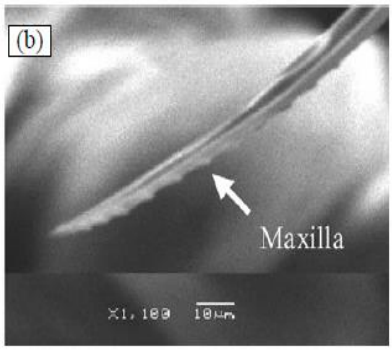

Painless because of highly serrated proboscis designed to reduce compression and nerve stimulation during a bite by increasing the efficiency of the cutting edge
Inside sheath:
Two tubes which enter the mosquito's unsuspecting prey.
1. Stylet is used to pierce through the skin and draw blood
2. Injects an anticoagulant into to keep the blood flowing.

Fig.1.1 Mosquito proboscis: (a) maxilla and labrum and (b) maxilla (Izumi et al., 2011))

There is a great variety of teeth that are evolutionarily adapted to the diet and predation habits. Each tooth exhibits micro-serrations along its cutting edge.

These serrations, approximately 10–15 μm in wavelength, are used to create a highly efficient cutting effect which converts some of the dragging force into normal force at localized points.

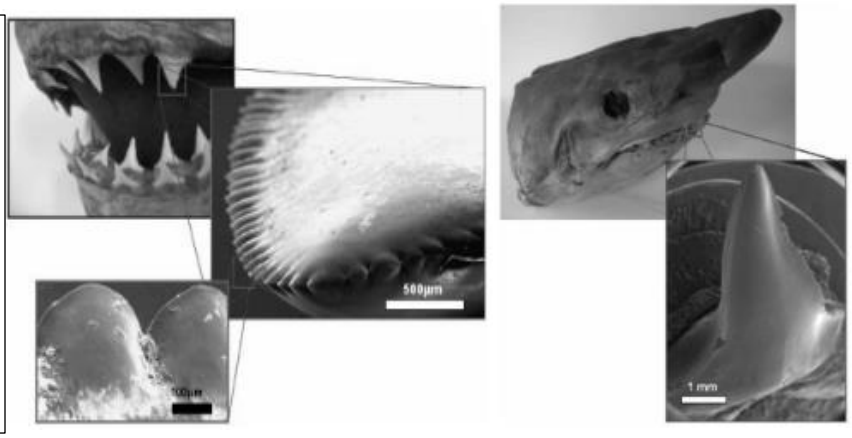

Fig.1.2. Great white shark (Carcaradon carcharinus) teeth (left) and a Mako shark and tooth (right)

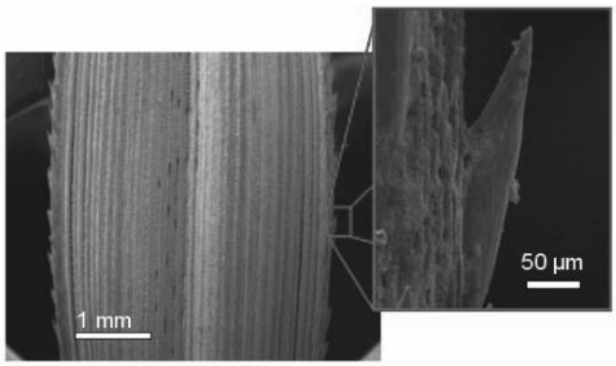

They extend approximately 50 µm from the body of the leaf and form sharp points with an apex angle of roughly 20˚. This sharp cutting edge was evolutionarily designed as a defense mechanism against grazing animals. This feature is also prominent in other grasses, such as Hypolitrium Shraderenium.

Fig.1.3. Pampas grass (Cortaderia selloana); note serrations at edges (right)

2.2. Literature review

There are many researches on bioinspired serrated cutting edges of biopsy bunches. Reducing the cutting pain and increasing the cutting accuracy are the primary objectives in this area. Dr. Giovannini designed and tested the cutting performance of a circular microserrated biopsy punches. Laser ablation was used to progressively ablate the tip of the biopsy cannula and eventually to get a circular cutting edge. The serrated profile is defined by three parameters: the radius at the tip, the arc radius, and the angle between two consecutive serrations. Specifically, they varied the arc radii from 50 to 600 micrometres and kept the radius at the tip unchanged. After manufacturing the microserration, a special testbed was designed to measure the insertion force, which attaches an amplifier to a piezoelectric dynamometer and then uses an NI data acquisition board to record the axial force. In a plot of axial force vs. displacement, the puncture force is defined as a peak force reached at the end of the deformation phase. As a result, a 30% maximum reduction of puncture force was achieved by one of the microserration configurations. [1] In summary, we were tasked to repeat the experiment with a different microserration profile and to investigate whether the new configuration will increase the cutting efficiency

3. Equipment setup

3.1 ND YAG Laser machine : Class IV

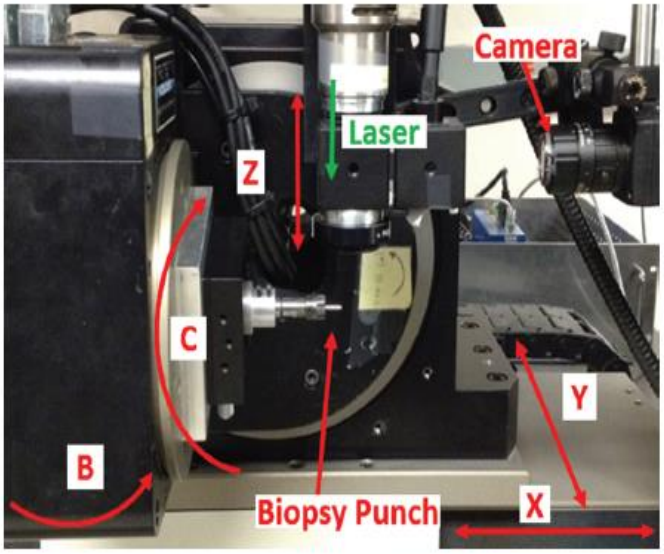

Fig.3.1. Laser system. The five axes of the positioning system (X,Y, Z, B, and C) and the main components of the laser system are highlighted. (Marco et al, 2017)

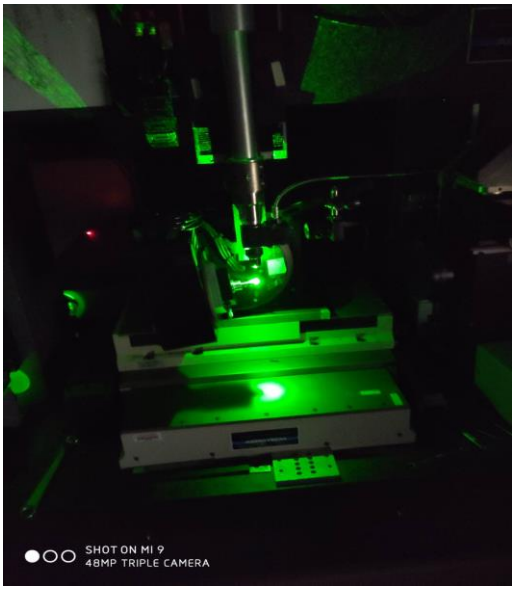

Fig.3.2. ND YAG Laser: Class IV

To perform the micro-cutting process on the tip of the biopsy punches, the ND YAG laser machine used. The picosecond laser system with the wavelength of 532 nm has 5 degree-of-freedom, including 3 linear translation (X, Y, Z) and 2 rotational motion (B, C). The repetition rate of the laser is chosen as 10kHz in order to get the maximum power during the cutting process. The motion of the 5 axes can be controlled manually or by a programmable controller with the resolution of 0.01 μm. The CCD camera is equipped to catch the image of the serration in micro-scale. The G code is attached in appendix, which was used to create 23 serrations on the tip of the biopsy punches.

The setup process mainly consists of 4 steps: (1) mount the square plate on the C axis (2) mount the black block on the square plate and this block relates to ER8 collet which is used to hold the biopsy punches. (3) fix the needle in the ER8 collet and fastening it tightly. (4) center the needle to make it be aligned with the C axis.

3.2 Alicona measurement:

Fig.3.3. Measuring the biopsy needle by using the Alicona machine

The Alicona machine has two main usage in this project: (1) measure the angle of the bevel. (2) view the serrations on the tip of the needle.

Since the laser is delivered vertically and its direction can not be changed, it is necessary to keep the surface of the working area horizontal all the time. The Alicona is used to measure the angle of bevel in micro-scale.

As shown in the Fig.2.4., the angle of the bevel is 14.6914°. This angle was used to control the rotation angle of the B axis of the laser system. The profile below is a cross-section image of the biopsy needle. The IF-Measurement software can automatically measure the angle starting from the green intersection to the red intersection.

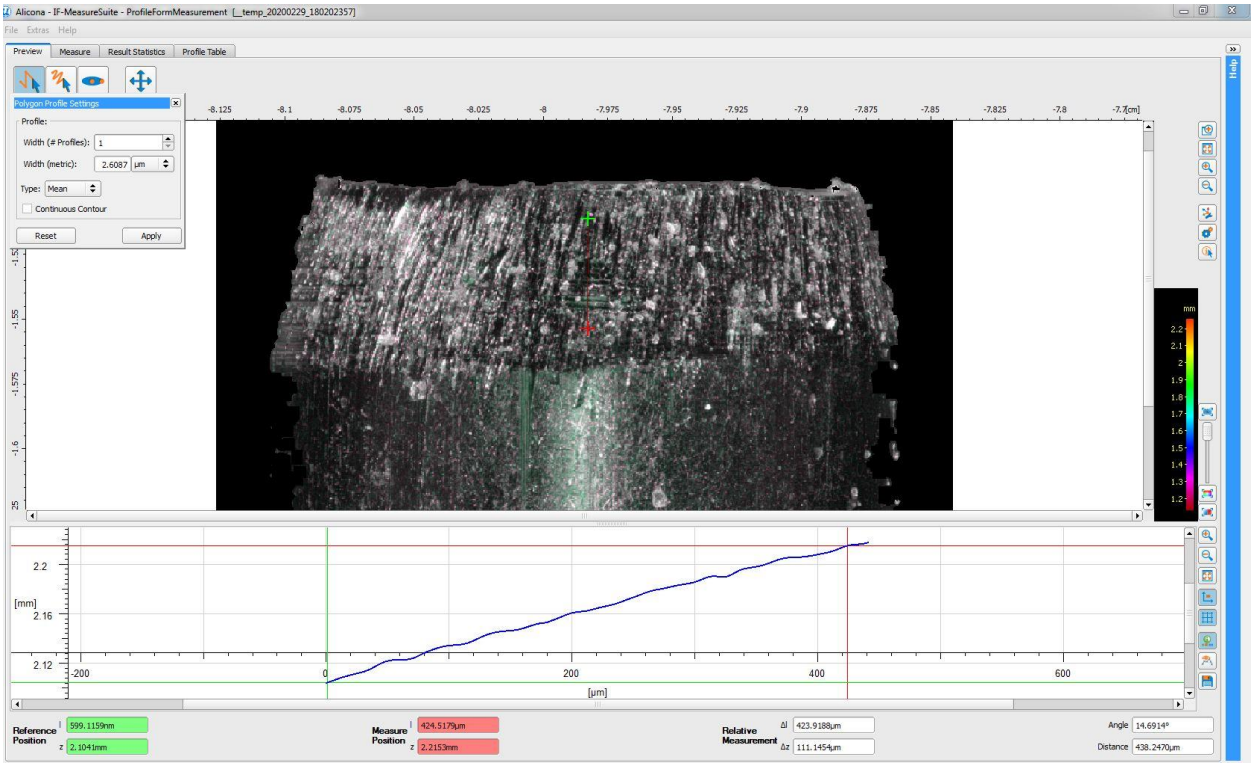

Fig.3.4. Angle measurement with the aid of Alicona

The other usage of the Alicona in this experiment is to help view the created serrations in micro-scale. In the Fig.3.5., the created serrations are shown, it is not perfect as proposed but it does improve the cutting performance of the needle.

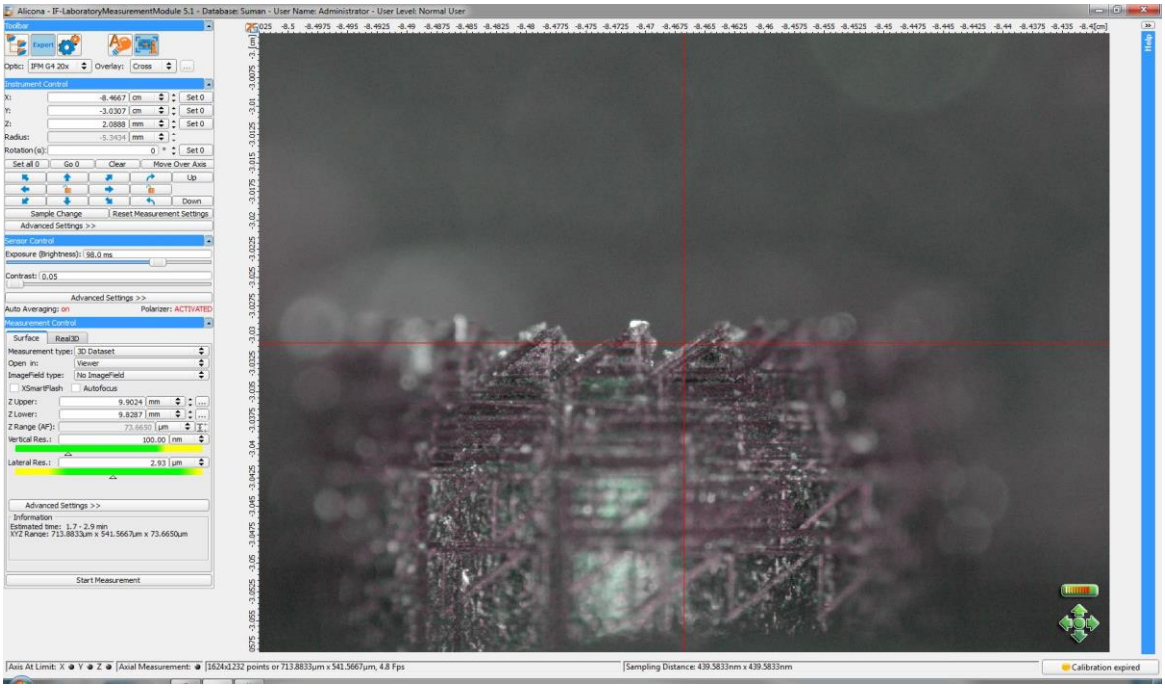

Fig.3.5. The image of the serrations on the biopsy needle (Alicona).

3.3 Insertion testbed:

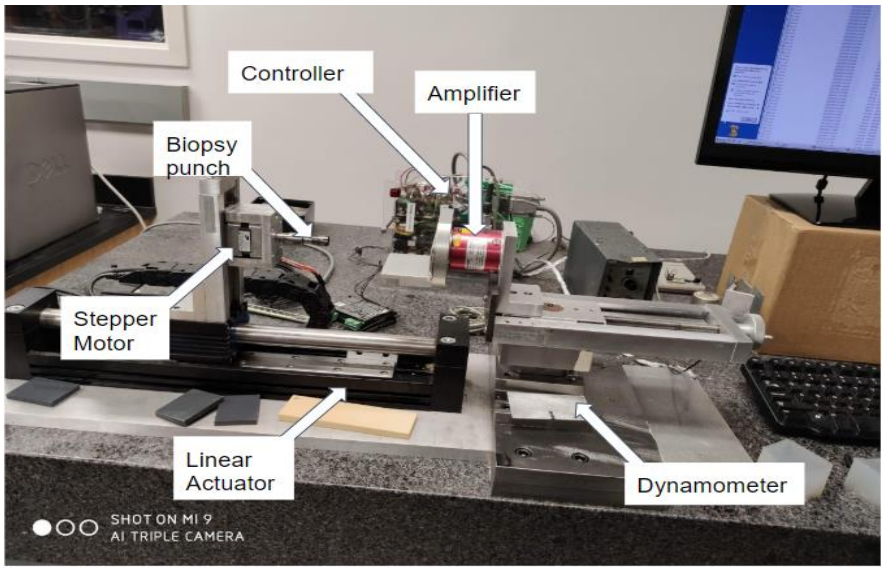

Fig.3.6. Insertion testbed

In the tests performed, the biopsy punch was mounted on the stepper motor through a customized fixture and a collet.

The linear actuator and stepper motor: axial motion and rotational motion of the biopsy punch.

- Resolution of the linear encoder is 12 lm with a maximal acceleration of 222 m/s2.
- Insertion force measurement: Kistler 9067 three-component piezoelectric dynamometer in conjunction with a Kistler charge amplifier.
- Force dynamometer sensitivity is 8 pC/N for the x- and y-axes, 3.8 pC/N for the z-axis.
- NI data acquisition board at a sampling rate of 1000 Hz.
- Duty cycle is chosen as 50% and the frequency is 254 Hz.
- The speed of the linear motion is 1mm/s.

The relationship between stepper motor frequency and rotational speed is:

$$Frequency = \frac{Vrotation}{\pi D} \times pulse$$

Since the diameter of the biopsy punche is 2 mm at the tip, the corresponding rotational speed is 4mm/s.

3.4 Phantom Tissue

Tissue mimicking materials are widely used in clinical simulators, medical research, and soft robotics. Within clinical simulators, materials that simulate the properties of real biological tissue are critical to make simulators more realistic for surgeons, nurses and caregivers to practice and learn their clinical skills.

Typically, soft PVC materials are made by combining a PVC polymer solution and its softener diethyl hexyl adipate, then heating the combination to a certain temperature. Components of the soft PVC material can be adjusted to design the new material with desired properties. For instance, the mass ratio between the softener and PVC polymer solution determines the hardness of the soft PVC material. By adjusting this ratio, the hardness of the soft PVC material can be changed to simulate the mechanical properties of different tissues

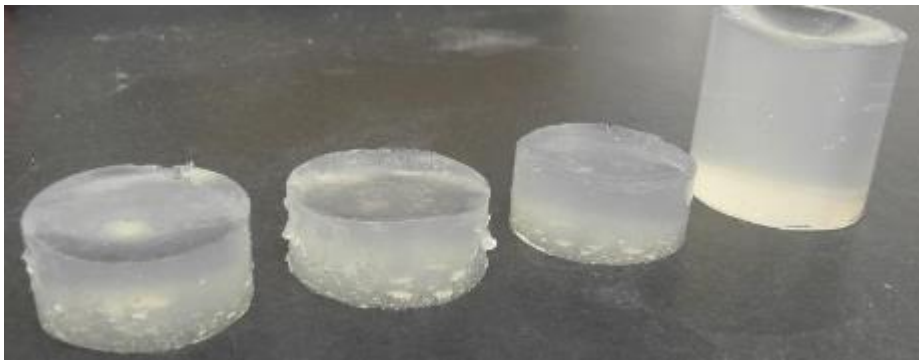

Fig.3.7. Phantom tissue sample developed by mixing **8116SS plastic with 4116S Plastic Softener** in a ratio **4:1**.

4. Design and machining path

4.1 CAD modelling and cutting analysis

Model - Cad file

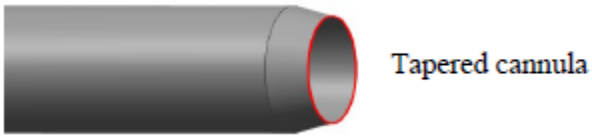

Fig 4.1 Standard cannula

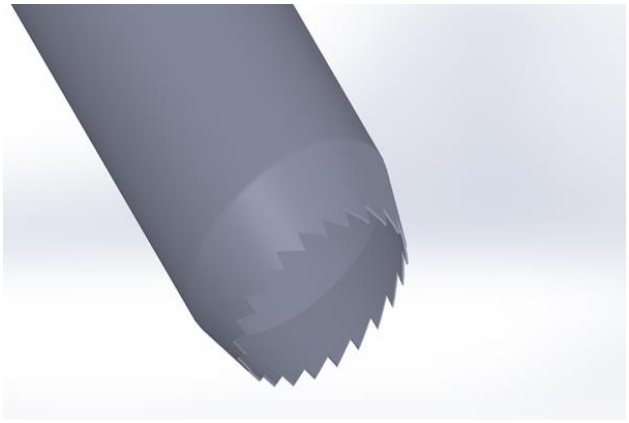

Fig.4.2. Orientation of the CAD model.

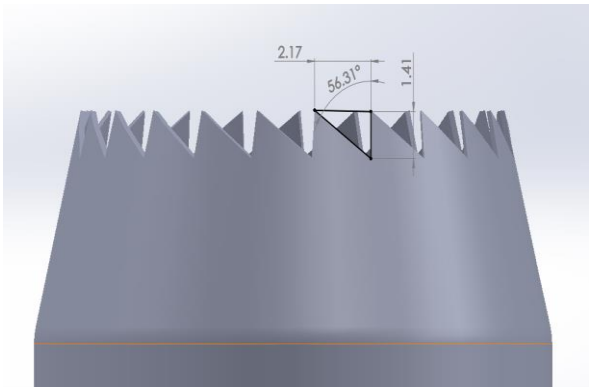

Fig.4.2. Dimensions of the model (Total number of serrations:23)

4.2 Machining tool path

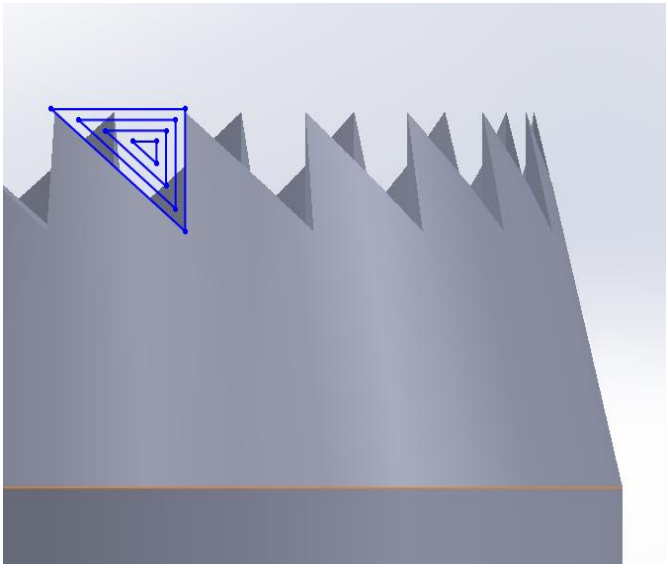

Fig.3.1. Tool path

The laser tool path used is progressively ablating the material, eventually leading to the generation of the desired features along the cutting edge of the biopsy punch.

An overlapp of 20% is considered when developing the machining path. This was done after understanding that the simple path along the profile would not give us the desired dimensional accuracy.

5. Theory

Fracture Mechanics Approach

Fracture Mechanics Approach. During the insertion of the biopsy punch, the puncture force can be analyzed by studying the fracture mechanics related to the BP insertion. According to the J-integral method, a crack will propagate inside the tissue when the energy generated by the insertion is equal or greater than the energy needed to extend the crack, where R is defined as the tissue fracture toughness, and it represents the energy required to propagate the crack.

The contact area(A) of serrated needles is lower than that of standard needles. Based on the equations shown below, it is inferred that the puncture force during insertions with micro-serrated BPs is reduced.

$$F \propto \sqrt[m]{\frac{R}{K}}\, A$$

$$\sqrt[m]{\frac{R}{K}}\, A_{SERR} < \sqrt[m]{\frac{R}{K}}\, A_{STAND}$$

6. Experiment results discussion

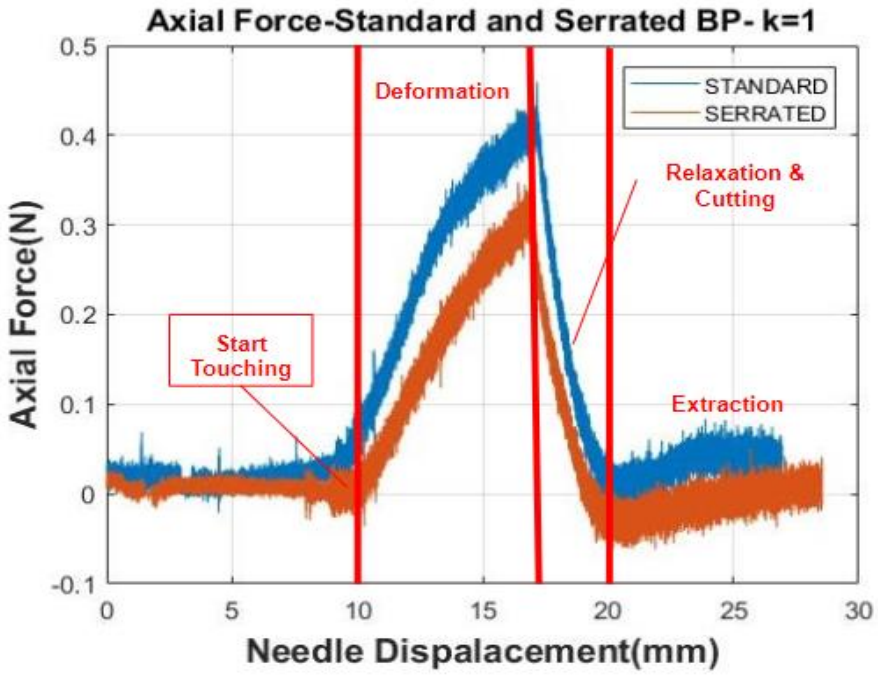

Fig.6.1. Comparison of the force between standard and serrated needles

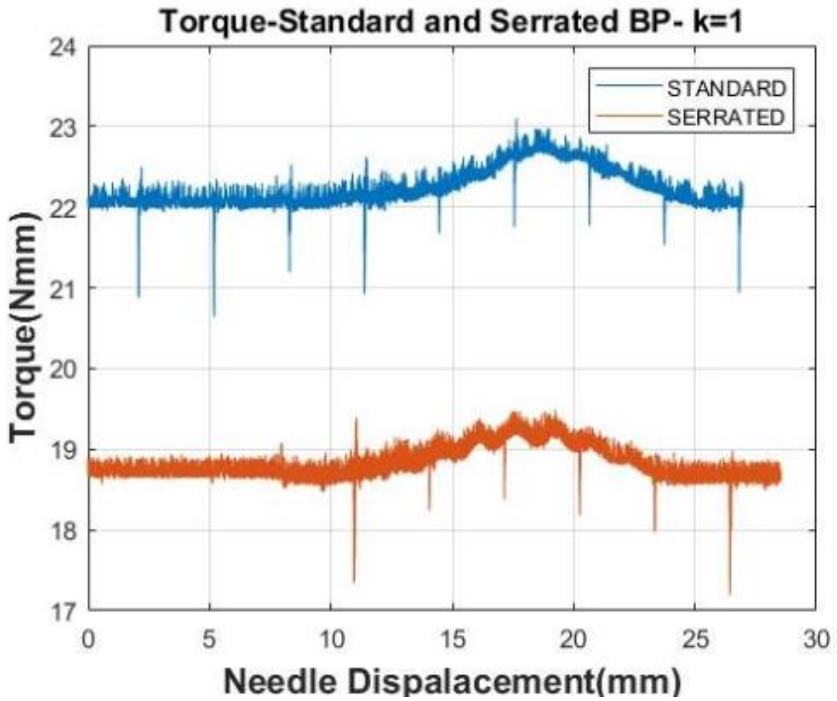

Fig.6.2. Comparison of the torque between standard and serrated needles

Example of maximum force and torque

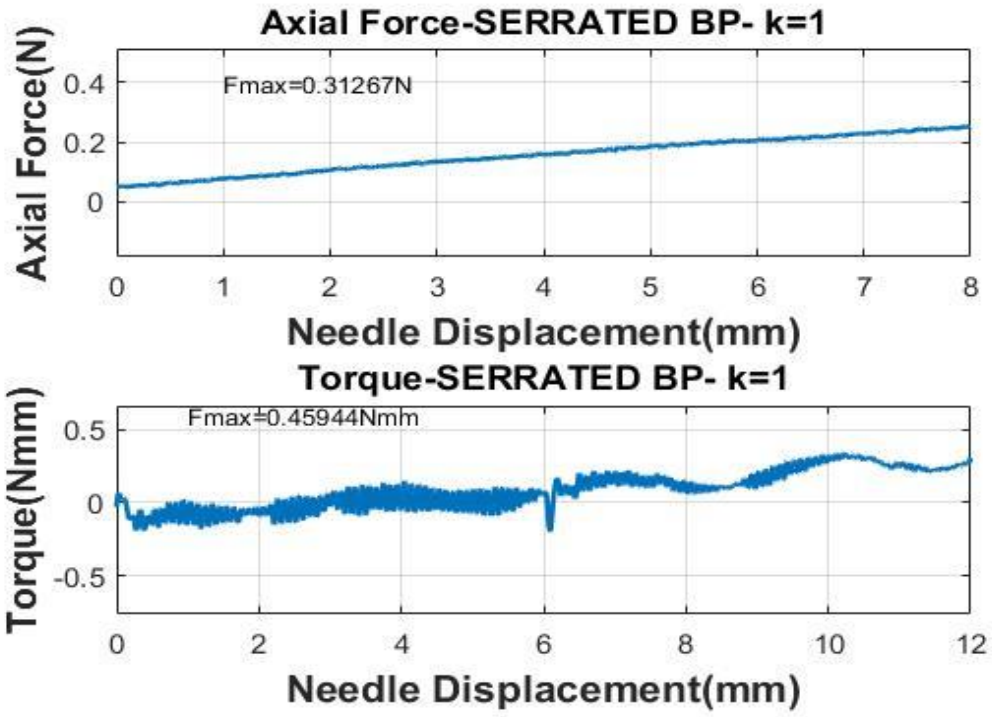

Fig.6.3. Maximum axial force and torque for serrated needle

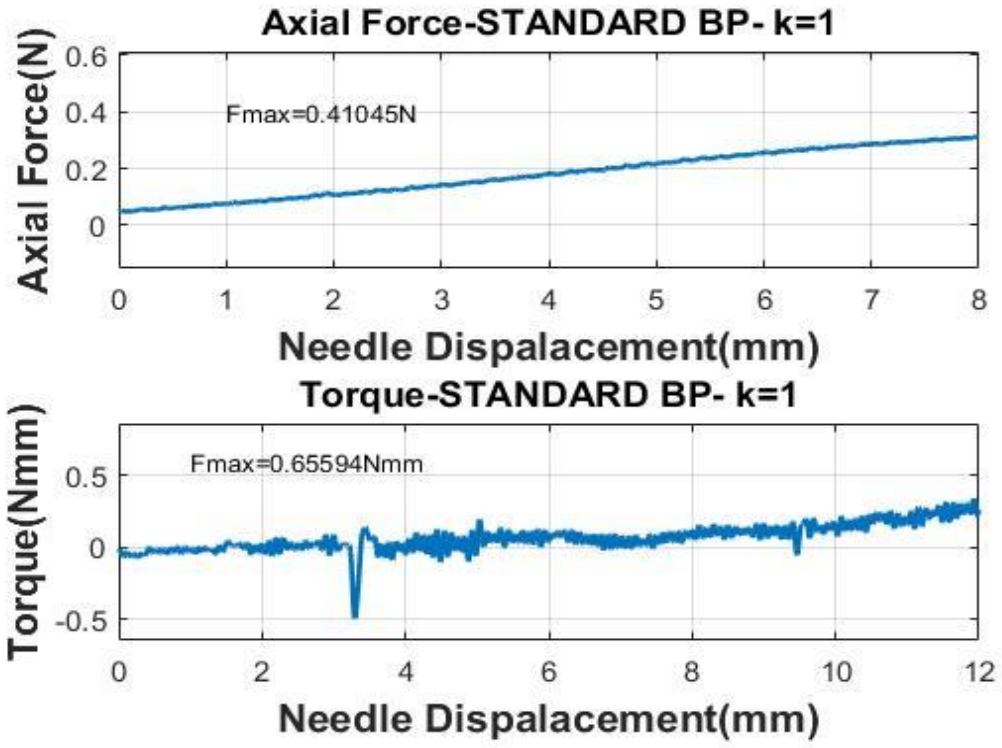

Fig.6.4. Maximum axial force and torque for standard needle

SERR AND STAND TESTING						
SERR #	Fmax(N)	Tmax(Nmm)		STAND #	Fmax(N)	Tmax(Nmm)
86	0.31718	0.55502		73	0.41045	0.65594
97	0.35781	0.59471		76	0.3979	0.63463
103	0.34505	0.57126		81	0.39272	0.6351
106	0.31267	0.45944		84	0.42733	0.66105

Fig.6.5. Statistical results for both type of needle

7. Challenge faced during the project

7.1 Needle centering

Centering tool with dial indicator (align with C axis).

Testing probe touches the needle surface. Readings shall be within the range of -30 to 30 while the needle is rotating.

7.2 Laser focusing

Changing the Z axis to get laser focused. Parallel nick on a horizontal surface to find the best Z position for the laser.

On Jan 31, Dr. Giovannini provided a detailed training on the laser machine with emphasis on the cannula mounting, operations on the machine tool. Following the training, we attempted to use the laser machine for machining the needle on two instances. We were unable to get the laser to focus effectively to bring about any significant material removal. In our trials we took suggestions from Suman to account for the material removed by changing the z height of the laser on each pass; to bring the laser back to focus. Other variations included change in the frequency of the laser beam, feed rate, number of passes.

8. Future work

8.1 Finite element computation

A computational analysis can be conducted in the future to understand the concept of high stress concentration on the surface of the skin which leads to fracture occurring much at lower insertion forces.

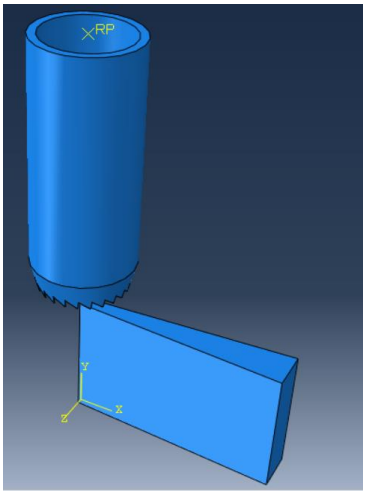

$$U = \mu \sum_{i=1}^{5} \frac{C_i}{\lambda_m^{2i-2}} \left(\bar{I}_1^i - 3^i \right) + \frac{1}{D} \left(\frac{J_{el}^2 - 1}{2} - \ln J_{el} \right),$$

where

$$C_1 = \frac{1}{2}, \quad C_2 = \frac{1}{20}, \quad C_3 = \frac{11}{1050}, \quad C_4 = \frac{19}{7050}, \quad \text{and} \quad C_5 = \frac{519}{673750}.$$

The shear behavior is described by the parameters μ and λ_m, while D governs the compressibility.

Fig.8.1. FEA analysis

Fig.8.2. Arruda-Boyce strain energy density function

The needle can be considered an analytical rigid body, whereas the tissue modelled as a hyperelastic material defined by the Arruda-Boyce strain energy density function, U as shown in figure 8.2.

The values are found to be **0.002,1.60, and 14.60**, respectively [12].

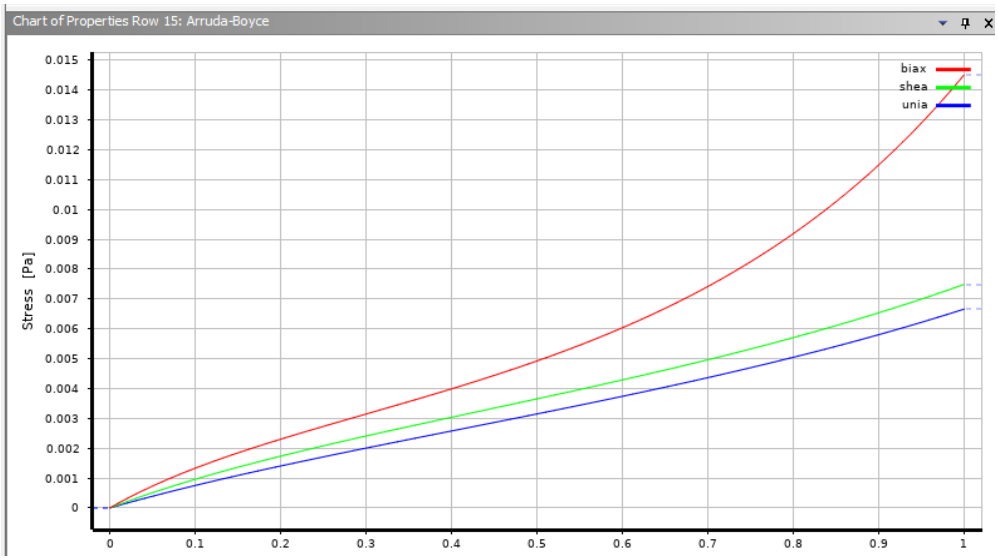

Fig.8.3. Hyperelastic curve for the phantom tissue

8.2 P value analysis

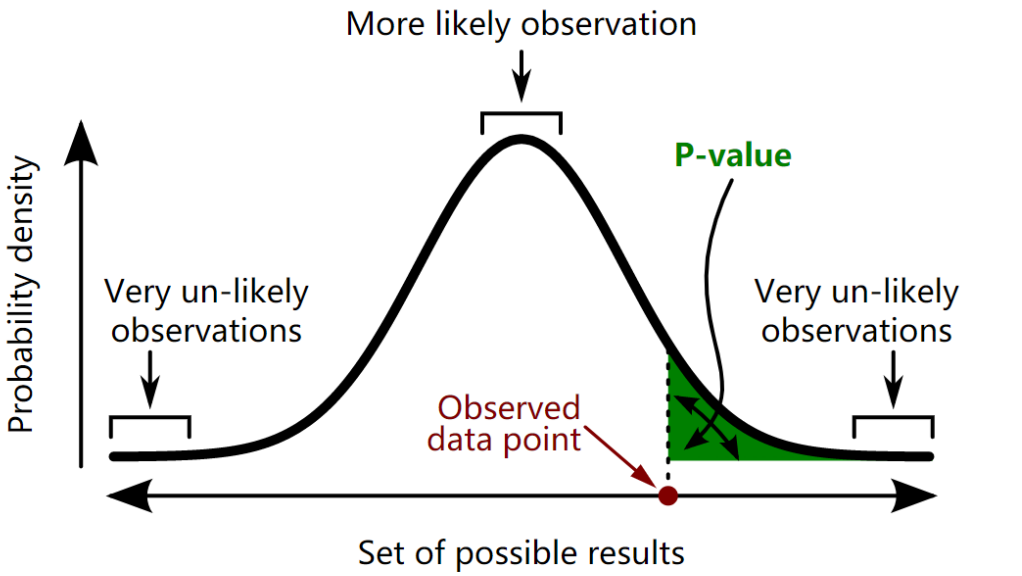

A **p-value** (shaded green area) is the probability of an observed (or more extreme) result assuming that the null hypothesis is true.

Fig.9.1 P-value analysis diagram

The *p*-value is defined as the probability, under the null hypothesis **H** about the unknown

distribution **F** of the random variable **X**, for the variate to be observed as a value equal to or more extreme than the value observed.

- $\Pr(X \geq x|H)$ for right tail event,
- $\Pr(X \leq x|H)$ for left tail event,
- $2\min\{\Pr(X \leq x|H), \Pr(X \geq x|H)\}$ for double tail event.

8.3 Echogenic placement

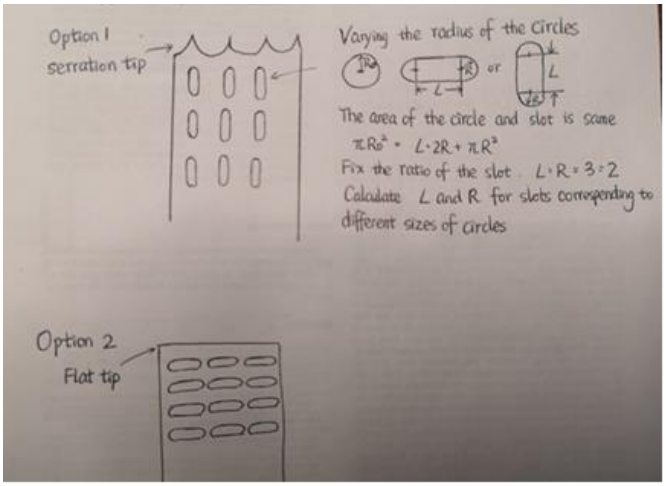

Optimisation for echogenic positioning

Strategies to increase needle visibility,

Development of echogenic needles, and advances in ultrasound imaging technology.

Echogenic needle design is an economic and reliable method of improving needle ultrasound visibility.

Micro-dimples, micro-corner reflectors, and micro-channels are often created near the needle tip to serve as ultrasound wave reflectors.

Basis for developing echogenic needles with lower insertion forces.

Inspiration from automobile industry.

Echogenic needle design is an economic and reliable method of improving needle ultrasound visibility. Micro-dimples, micro-corner reflectors, and micro-channels are often created near the needle tip to serve as ultrasound wave reflectors. Basis for developing echogenic needles with lower insertion forces. Inspiration from automobile industry to reduce friction forces in bearings, cylinder pistons, etc.

9. Appendix

9.1 G Code:

```
$beam_dia = 0.01
$radius = 0.0825
$overlap = 0.99
$overlap_R = 0.80
$dist_R = (1-$overlap_R)*$beam_dia
$depth=0.005
$feed=0.12
$pass1=23
$pass2=50
$pass3=20
$pulse_time= (((1-$overlap)* $beam_dia*1000000)/$feed
$tex=0.0025
G91
G92 X00 Y0 Z0 C0

PSOPULSE X TIME $pulse_time ($pulse_time/2) cycles 5000000
REPEAT $pass1

REPEAT $pass2

REPEAT $pass3
$over1=0
        REPEAT $pass2

                        PSOCONTROL X FIRE
                        G01 Y 0.2262 -$over1 F $feed
                        G01 X (-0.28+(2*$over1)) Y (-0.2262 +$over1) F $feed
                        PSOCONTROL X OFF

                        G01 X (-0.28-2*$over1) F 1
```

9.2 Working log

1. Jan 27 A training was provided by PhD student Suman Bhandari on the basic operation of the laser machine and essentials safety precautions.
2. On Jan 31, Dr. Giovannini provided a detailed training on the laser machine with emphasis on the cannula mounting, operations on the machine tool.
3. Feb First session on the laser machine. We determined how to focus the laser
4. Feb 7th Second attempt. We tried various possibilities
5. Feb 13th Third attempt on machining. The machining was not so effective. Was done in the presence of Dr. Giovanni
6. Feb 20th Fourth attempt. Needle dimension reduced to 20mm, 2mm thickness. Laser machine had lost power since the repair to Germany.
7. Feb 21-22 Pass criteria changed. First serration accomplished after 1 hour. Weekend machining, 12 hours helped accomplish goal 50 percent material removal
8. Feb 29-29-March 1: serrations completed. However the material is not completely removed.
9. March 1st Training on force measurement machine

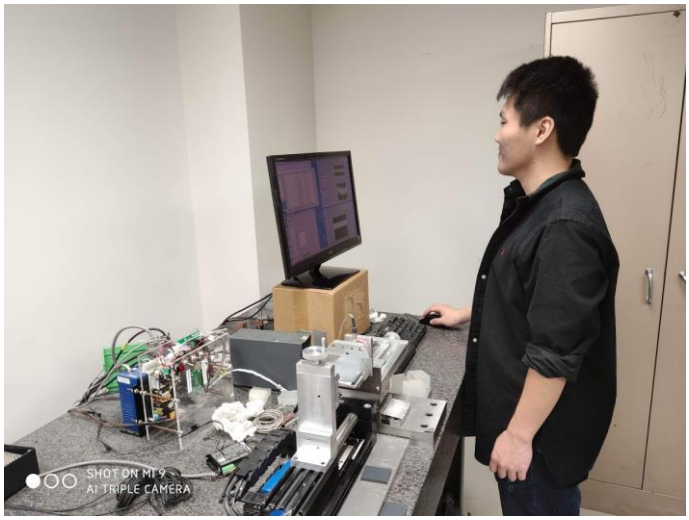

10. Bibliography

A Generalized Analytical Model of the Cutting Angles of a Biopsy Needle Tip. Kornel Ehmann , Kostyantyn Malukhin

Study of the effect of cannula rotation on tissue cutting for needle biopsy. Han P, Ehmann K.

Bioinspired microneedle insertion for deep and precise skin penetration with low force

Design and models of helical needle geometries for core biopsies. Marco Giovannini, Jian Cao, Kornel Ehmann

Vibration-assisted slicing of soft tissue for biopsy procedures. Marco Giovannini, Xingsheng Wang, Jian Cao, Kornel Ehmann

Study on design and cutting parameters of rotating needles for core biopsy. Giovannini M, Ren H, Cao J, Ehmann K.

P. Guo, K. Malukhin, K. Pallav, and K. Ehmann. "The Geometry, Manufacture, and Performance of Biopsy Needle Tips", 01/01/2010-12/31/2010, 2010, "Proc. Int. Conf. on Micromanufacturing - ICOMM-2010, UW-Madison WI, April 2010"

Needle Biopsy Adequacy in the Era of Precision Medicine and Value-Based Health Care. Archives of Pathology & Laboratory Medicine

Contributions in medical needle technologies—Geometry, mechanics, design, and manufacturing. Yancheng Wang, Weisi Li, Peidong Han, Marco Giovannini, Kornel Ehmann & Albert J. Shih

Effects of needle inner surface topography on friction and biopsy length. Weisi Lia,b, Ping Zhoua, Wei-Chen Linb, Valens Nteziyaremyec, Hitomi Yamaguchic, Dongming Guoa, Albert Shihb

Modeling of machined depth in laser surface texturing of medical needles. Xingsheng Wanga,b, Peidong Hanb, Marco Giovanninib, Kornel Ehmann

12. Han P., Mechanics of Soft Tissue Cutting in Needle, Insertion PhD Thesis, Northwestern University, May 2014.

21. The Cutting Edge: Sharp Biological Materials* M.A. Meyers, A.Y.M. Lin, Y.S. Lin, E.A. Olevsky, and S. Georgalis

22. Biomimetic Mosquito-Like Microneedles

23. Laser surface texturing of medical needles for friction control

11. Acknowledgements

We acknowledge the help of Prof. Ehmann, Dr. Giovannini, Suman Bhandari and Bella for the project.

A special thank to Dr. Giovannini to be extremely patient in training us and guiding us through the course and also providing the necessary motivation to continue in the face of challenges.